Mechanical Properties of Hysol EA-9394 Structural Adhesive

RECEIVED

MAR 1 5 1995

O S T I

T. R. Guess, E. D. Reedy, M. E. Stavig

SF2900Q(8-81)

DISCLAIMER

Portions of this document may be illegible in electronic image products. Images are produced from the best available original document.

MECHANICAL PROPERTIES OF

HYSOL EA-9394 STRUCTURAL ADHESIVE

T. R. Guess, E.D. Reedy, and M. E. Stavig

Sandia National Laboratories

Albuquerque, NM 87185

ABSTRACT

Dextor's Hysol EA-9394 is a room temperature curable paste adhesive that is representative of the adhesives used in wind turbine blade joints. A mechanical testing program has been performed to characterize this adhesive. Tension, compression stress relaxation, flexural, butt tensile, and fracture toughness test results are reported.

MASTER

INTENTIONALLY LEFT BLANK

INTRODUCTION

Composite-to-metal tubular lap joints are used in applications ranging from joining composite drive shafts to metal end fittings in automobiles to joining composite blades to metal hubs in wind turbines. These joints are often held together with a structural adhesive. Because wind turbine joints have been observed to fail short of their design life, studies have been conducted to gain an understanding of the static and fatigue behavior of tubular composite-to-metal joints [1-3]. Hysol EA-9394 structural adhesive was used in the joints that were tested and analyzed in these studies. Analysis of such joints require a knowledge of the mechanical behavior of the adhesive. Tension, compression stress relaxation, flexural, butt tensile, and fracture toughness tests were performed to characterize the Hysol EA-9394 adhesive. Experimental procedures and results are presented in this test report.

MATERIAL

Dexter Corporation's Hysol EA-9394 is an amine-cured epoxy paste adhesive with an aluminum powder filler. This adhesive combines high temperature performance with strength and toughness; it can be cured at room temperature. Specimens in this study are cured at room temperature for a minumum of seven days prior to testing and all mechanical tests are performed at room temperature ($\approx 22°C$). The adhesive has a density of 1.38 g/cc, a porosity of about 6%, a glass transition temperature of 82°C and a coefficient of thermal expansion of approximately 60 x 10^{-6} °C^{-1} (between -30°C and 70°C).

Scanning Electron Microscope (SEM) inspection of fracture surfaces reveals that our specimens contain porosity throughout (Figure 1). Comparisons between the microstructure of EA-9394 samples prepared at SNL/NM and those prepared at Hysol show that the microstructrues are very similar; no distinct differences are detected. Based on these results, we conclude that SNL/NM is processing the adhesive correctly and that the material inherently contains porosity throughout. Even with this porosity, EA-9394 performs as advertised.

EXPERIMENTAL PROCEDURES AND RESULTS

TENSION

Static Tests

Flat dogbone tension specimens are molded to final nominal dimensions of 6.5 inches length, 0.75 inch width, and 0.20 inch thickness. In the reduced-size gage section the width is 0.5 inch and length is 2.25 inches. Specimens are instrumented with a 2.0-inch extensometer in the gage section to measure strain. Testing procedures follow the guidelines in ASTM D-638, the Standard Method of Test for Tensile Properties of Plastics. Tensile loads are introduced into the specimens by means of wedge grips with serrated faces using a screw-driven Model 1125 Instron test machine. Crosshead speed is 0.09 inch/minute; this translates into a strain rate of approximately $0.0003s^{-1}$. All tension tests are performed at room temperature to stress values below 6300 psi. A typical tensile stress-strain curve is shown in Figure 2; the response is nonlinear. Initial elastic moduli are taken as the tangent values of the stress-strain curves between 100 psi and 1500 psi; these moduli are listed in Table 1.

COMPRESSION

Stress Relaxation Tests

Adhesive compression stress relaxation behavior is measured using strain-gaged, cast cylindrical specimens (height/diameter = 2) tested in axial compression. Testing procedures follow the guidelines in ASTM D-695, the Standard Method of Test for Compressive Properties of Rigid Plastics. Specimens of 1.13 inches height and 0.56 inch diameter are placed in a subpress within an Instron test frame to minimize misalignment. In the stress relaxation tests, specimens are first loaded to some fraction of the compression yield strength. Crosshead displacement is then held constant while stress decay is monitored for thirty minutes. Following the thirty minute hold, those specimen initially loaded to yield are reloaded until the material yields for the second time. Figure 3 shows a typical stress-strain response of a specimen with an initial loading rate of $0.0003 \, s^{-1}$ and a second loading at $0.003 \, s^{-1}$ after the thirty minute stress relaxation.

The stress relaxation tests are used to obtain stress-strain responses as well as time dependent stess relaxation. Typical compression stress-strain responses to yield are shown in Figure 4 for specimens loaded at strain rates of 0.003, 0.0003, and 0.00003 s^{-1}. Yield strength is defined as the peak stress attained during compression loading. These curves display substantial nonlinearity prior to maximum stress. Compression yield strength, initial modulus and Poisson's ratio data are listed in Table 2. Three different strain rates are used for the initial loading of the specimens loaded to yield; however, these specimens are all reloaded at a single strain rate. Stress-time histories for specimens initially loaded at three different strain rates and reloaded at $0.003s^{-1}$ are shown Figure 5. Stress-time histories for specimens initially loaded to 25%, 50%, 75%, and 100% of yield strength are illustrated in Figure 6.

Table 2 data shows that on initial loading Hysol EA-9394 has an average Young's modulus of about $0.59x10^6$ psi and a Poisson's ratio of 0.37. Initial yield stress increases with increasing strain rate from σ=9250 psi at ε=0.00003 s^{-1} to σ=11,400 psi at ε=0.003 s^{-1} . On second loading at a strain rate of $0.003s^{-1}$, following the 30 minute hold, the compression peak stress reaches a value of about 12,400 psi, $\approx$9% greater than the11,400 psi yield strength for an initial loading with the same strain rate. Figure 6 illustrates the magnitude of stress relaxation for specimens initally loaded to different fractions of yield. After a 30 minute hold on crosshead displacement, compressive stresses decay by about 34%, 17%, 7% and 6% in specimens initially stressed to 100%, 75%, 50% and 25% of yield, respectively. These results suggest a nonlinear viscoelastic behavior. As the applied stress approaches the yield strength, stress relaxation is increasingly pronounced.

FLEXURE TESTS

Testing procedures for four-point bending tests follow the guidelines in ASTM D-790, the Standard Test Methods for Flexural Properties of Plastics and Electrical Insulating Materials. Hysol EA-9394 bars of 0.50 inch width and 0.20 inch thickness are loaded in four-point bend using support and load spans of 3.0 and 1.0 inches, respectively. Biaxial strain gages are bonded to the tension and compression surfaces; a crosshead speed of 0.17 inch/minute produces a flexural strain rate of about $0.0003s^{-1}$ in the specimen. Typical flexural moment-strain responses

on the tension and compression surfaces are shown in Figure 7; values of initial flexural modulus and Poisson's ratio are listed in Table 3. These curves suggest yield on the tensile side first and a tensile yield strength lower than the compression yield strength. Values of flexural modulus (Table 3) are slightly higher than the tensile and compressive moduli (Tables 1 and 2) for specimens loaded at identical strain rates of $0.0003s^{-1}$; values of flexural Poisson's ratio are slightly lower.

BUTT TENSILE TESTS

Butt tensile tests are conducted to complement modeling studies of the strength of bonded joints [4,5]. This reference used a relation defining the interface corner stress intensity factor K of an idealized butt joint composed of a thin, brittle (linear) adhesive layer fixed between rigid adherends and subjected to a transverse tension loading to predict joint failure. This relation indicates that if failure ocurs at a critical K value, joint strength should vary as the reciprocal of the cube root of bond thickness. Butt joints fabricated using a brittle unfilled adhesive have been tested, and measured strengths of these joints do show the predicted thickness effect [4,5]. Joints fabricated using a more ductile adhesive, the Hysol EA-9394, show relatively less variation in joint strength with bond thickness. The Hysol EA-9394 butt joint tests are described in the following section.

Butt tensile specimens are used to measure joint strength as a function of adhesive bond layer thickness. In essence, the joint specimen bonds two 303 stainless steel rods end-to-end with a layer of Hysol EA-9394 epoxy adhesive. The stainless steel rods (adherends) are solid cylinders (1.13 inches diameter by 1.5 inches length) that have been precision machined to guarantee that the ends are flat and perpendicular to the cylinder axis. A transverse hole drilled through each adherend is used to pin completed specimens into a load train for testing.

Butt tensile joint specimens are assembled using fixtures specially designed to ensure alignment of the two adherends and precise control of the adhesive layer bond thickness. Major components of the fixturing are a V-block to ensure axial alignment of the adherends, an aluminum holder to secure the V-block and a digital micrometer for setting bond thickness. The ends of adherends are sandblasted and then chemically cleaned prior to bonding. Chemical

8

cleaning consists of a trichloroethylene rinse followed by an alcohol wipe and then air blow drying. Thickness of the bond layer is determined by calculating the difference between the final specimen length and the initial total length of the two adherends.

Static and stress rupture butt tensile tests on specimens with nominal bondline thicknesses of 0.025, 0.050. and 0.100 inch were conducted in a 100,000 pound capacity electrohydraulic load frame. The load train utilizes a chain linkage attached to the specimen via a pinned clevis. The static failure tests are loaded at a crosshead displacement rate of 0.5 in/minute, with a time to failure ranging between 15 and 19 seconds. The measured ratio of failure stress to time to fail is on the order of 400 psi/s. Stress rupture specimens are quickly loaded ($\cong$ 12 s) to either 74%, 82% or 90% of static failure and the load is sustained until the bond fails or until the test is terminated by increasing the load to measure residual strength.

Butt tensile test results are listed in Table 4 and plotted in Figures 8-10. Static joint strength displays moderate variability (standard deviation/average ratio $\cong$ 7-14%). This variability is not large enough, however, to obscure the dependence of measured static joint strength on bond thickness as shown in Figure 8. The strength decreases by about 20% as bond thickness increases from 0.025 inch to 0.10 inch. Interestingly, the residual strength of joints subjected to sustained loading increased with the time under load (Table 4 and Figure 9). Times to failure as a function of applied stress are shown in Figure 10. For a prescribed stress level, the joints with the thicker bonds fail first. The results suggest that a joint with a 0.05 inch bond should not be subjected to a stress exceeding 70% of the static strength if it is to survive at least three hours.

Fractography examination of the failed joints indicates that failure always initiates adhesively (on the interface) along a small segment of the specimen periphery. This region of adhesive failure reaches no more than 0.20 inch into the specimen interior. Beyond this region, the failure is completely cohesive. This observation is consistent with failure initiated by high interface corner stresses.

FRACTURE TOUGHNESS TESTS

Fracture toughness is a measure of a material's ability to resist crack propagation. A single-edge-notched (SEN) specimen is used to measure the Mode I (opening mode) fracture toughness

of bulk Hysol EA-9394 adhesive. An adhesively bonded end-notched-flexure (ENF) specimen is used to measure the Mode II (shear) static and fatigue critical energy release rates of the Hysol EA-9394 adhesive.

Single-Edge-Notched (SEN) Tests

Fracture toughness parameters for the bulk Hysol EA-9394 adhesive are obtained from three-point bend tests on single-edge-notched specimens (see Figure 11). Linear elastic fracture mechanics (LEFM) can be used to characterize the onset of Mode I crack growth from a pre-existing crack as discussed in ASTM E-399, the Standard Test Methods for Plane Strain Fracture Toughness of Metallic Materials. This standard places a linearity criterion on the load-displacement response for the test to be valid; it will be shown that the EA-9394 specimens meet the linearity requirement. The Mode I stress intensity factor K_I describes the state of stress in the vicinity of the tip of a crack as a function of specimen geometry, crack geometry and applied load. The load P at which a crack propagates from a pre-existing crack is used to determine K_{IC}, the Mode I fracture toughness. An analytical expression for a single-edge-notched isotropic elastic specimen in three-point bending is given in ASTM E-399:

$$K_{IC} = [P_{max}S / t \, d^{1.5}] \, f(r) \tag{1}$$

$$f(r) = 3r^{0.5} [1.99 - r(1-r)(2.15 - 3.93r + 2.7r^2)] / [2(1 + 2r)(1 - r)^{1.5}] \tag{2}$$

where P_{max} is the maximum load, S is the span, t is specimen thickness, d is specimen depth, a_0 is initial crack length, and $r = a_0/d$ is the ratio of initial crack length to specimen depth.

A sharp precrack is produced on one edge of rectangular bars of Hysol EA-9394 (t = 0.235 inch and d = 0.498 inch) using a procedure in which the sample is clamped, a single-edge razor blade is placed against the specimen and a 150 gram weight is dropped from a set height onto the razor blade. The resulting natural crack extends beyond the tip of the blade. The length of the precrack on each side of the specimen is measured by an optical comparator and the average of the two values is the initial crack length a_0 used in Eq. (2). An Instron 8511 electrohydraulic

10

machine, equipped with a three-point bend fixture is used to input and record the load to break. The support span S is 2.0 inches. Specimen mid-span lateral deflection is measured as a function of applied load using an extensometer attached between the loading ram and the bend fixture.

A typical load-deflection curve is shown in Figure 12 and values of Mode I fracture toughness K_{IC} are listed in Table 5; the average value of K_{IC} is 1944 psi in$^{0.5}$. These are valid Mode I plane strain K_{IC} values according to the procedure in section 9.1.1 is ASTM E-399. A line with a slope of 0.95 times the initial slope intersects the load-deflection curve at or after the maximum load has occurred (see Figure 12). Satisfying this criterion results in a valid test for plane strain fracture toughness testing. For comparison, the critical fracture toughness K_{Ic} of 828/T-403, a room-temperature cured, unfilled epoxy, is 680 psi in$^{0.5}$.

End Notch Flexure (ENF) Tests

The purpose of the ENF specimen is to determine the critical energy release rate in a pure Mode II (shear) loading. This specimen is reported to produce shear loading at the crack tip without introducing excessive friction between the crack surfaces [6]. The ENF geometry was selected to investigate failure in the bondline of a composite-to-metal joint. The geometry of the ENF specimen is shown in Figure 13.

For a bimaterial beam where the contribution of the adhesive layer is neglected, i.e., a rigid interface between the two adherends, it can be shown using simple beam theory and the definition of the J-integral that

$$G = (1/2w) \, (Pa_0/2)^2 \, [(1/((EI)_{top} + (EI)_{bottom}) - 1/(EI)_{UC})] \qquad (3)$$

where P is the load, w is the specimen width, a_0 is the initial crack length, $(EI)_{top}$ is the effective bending stiffness of the top adherend (eg, the composite), $(EI)_{bottom}$ is the effective stiffness of the bottom adherend, and $(EI)_{UC}$ is the effective stiffness of an uncracked specimen. Calculations indicate that when the composite is on top, the crack closes and the critical energy release rate G_C = G_{IIC} (assuming frictionless contact), where II indicates Mode II shear loading. When the aluminum layer is on top a mixed Mode I and Mode II loading occurs.

The ENF specimen consists of two dissimilar adherends and an adhesive bond. One adherend is an E-glass/polyester woven fabric composite (E_{warp} = 4.1 x 10^6 psi and E_{fill} = 2.8 x 10^6 psi), and the second adherend is 7075 aluminum (E = 10 x 10^6 psi); both adherends are 0.25 inch thick. The warp direction of the composite is parallel to the long axis of the specimen. The bondline is Hysol EA-9394 epoxy adhesive of nominal 0.018 inch thickness. Sandwich plates (8 inch by 8 inch) from which individual specimens are machined are initially fabricated and cured at room temperature in a press. The aluminum surface is prepared for bonding with a light sandblast followed by cleaning with a trichloroethylene rinse, an alcohol wipe and blow drying; the composite surface is lightly sanded by hand then chemically cleaned in the same manner. Adhesive is placed between the two plates and final bondline thickness is controlled by pressing to stops.

An initial crack is required in the bondline on one end of the specimen. A sharp natural crack is required and tests were performed on samples in which the initial crack was produced by three different methods. The first is to use a thin slitting saw to cut an ≈0.014 inch wide notch of ≈1.0 inch length into the bondline, then extend as a natural crack by wedging open the bondline. The second method uses a sawn coarse crack that is extended as a natural crack by fatigue (cyclic) loading at 5 Hz in three-point bending. A third method that was tried for producing a natural crack is to use a razor blade to wedge open the specimen without a prior saw cut in the bondline. This last method was not successful in starting the crack in the adhesive or along the interface between the adhesive and composite. The crack developed in the composite near the interface, possibly due to low interlaminar strength of the composite.

Static and fatigue ENF tests were performed in a three-point bend fixture with a support span is 4.0 inches. The initial crack length a_0, as defined in Figure 13, is either 1.0 or 0.875 inch. Static tests are those in which the specimen is taken to failure (crack extension occurs) on the first loading cycle at a crosshead speed of 0.05 inch per minute. Fatigue tests are those in which the specimen is cycled at 5 Hz between maximum and minimum loads (R=.10) that do not produce crack extension on the initial loading cycle. Changes in specimen compliance and visual inspection are used to monitor crack growth as a function of loading cycles. Both sides of each specimen are painted with a thin coat of white paint (water soluble whiteout); a 6x/40x

microscope is used to periodically inspect for crack extension during a test. Time, number of cycles, specimen mid-span deflection, and load are recorded for each test.

Static ENF specimens fall into six groups that are distinguished by specimen orientation and method used to produce the pre-existing crack. Description of the groups and static test results are listed in Table 6. The critical strain energy release rate G_{IIC} is calculated from Eq. (4) using specimen dimensions and material properties, the length of the crack a_0 from the support point to the crack tip, and the maximum load. It was decided to use group 5 type specimens for ENF fatigue tests. In this group, the natural crack is extended from a saw cut by 5 Hz cyclic loading at a calculated G_{II} value of 290 J/m^2, which is about 35% of G_{IIC} measured in the group 5 static tests. It took between 150 and 750 cycles to grow a natural crack about 0.35 inches beyond the saw cut.

An objective of the ENF fatigue tests is to determine if this test method can be used to characterize resistance of the bimaterial joint to cyclic loading at levels below the static strength (or G_{IIC}) of the joint. A plot of G vs. N, where N is the number of cycles, will be indicative of the fatigue resistance of the specimen. The testing approach is to cycle ENF specimens at 5 Hz with the specimens being loaded to peak G_{II} values ranging from 200 J/m^2 (250 pounds load) to 460 J/m^2 (375 pounds load). Recall that the group 5 specimens in static tests had an average critical strain energy value G_{IIC} of about 860 J/m^2. The load and mid-span deflection is recorded for every 500th cycle until the test is terminated because either the crack is not growing beyond the initial crack tip or the crack has grown more than 0.10 inches beyond the initial crack tip.

An analysis of the compliance of the bimaterial ENF specimen in 3-point bending indicates that for an initial crack length a_0 of 0.875 inch, a change in crack length of 0.10 inch corresponds to a change in mid-span deflection of 0.0005 inch. This analytical result, which is in agreement with experimental compliance values of the ENF specimen, is used to analyze and interpret the fatigue data. That is, the mid-span deflection versus number of fatigue cycles is examined to find the number of cycles N at which the change in mid-span deflection equals 0.0005 inch (and the crack is assumed to have extended 0.10 inch). This value of N is then defined as the critical number of cycles to initiate crack growth for the applied G_{II} value. If the change in mid-span deflection is less than 0.0005 inch when the test is terminated, the test is a 'runout' and is

defined to have no crack growth for the number of cycles in the test. Group 5 type specimen ENF static and fatigue test results for are listed in Table 7 and the results are plotted in Figure 14.

The data are limited, however, it appears that the approach described may have merit for examing the fatigue resistance of interlaminar crack growth in bimaterial joints of the type found in wind turbine blades. Changes in beam compliance can be easily detected by monitoring specimen mid-span deflection during cyclic loading. Such changes in compliance are indicative of crack extension resulting from fatigue loading.

CONCLUSIONS

The mechanical tests on Hysol EA-9394 structural adhesive indicate:

1) Initial tension and compression moduli are about 0.60×10^6 psi and Poisson's ratio is 0.37.

2) Yield strength is strain rate sensitive and increases from 9,250 to 11,400 psi as the strain rate increases from 0.00003 to 0.003 s^{-1}.

3) The adhesive exhibits nonlinear viscoelasticity with significant stress relaxation occuring when stress levels approach the material yield strength (34% drop in stress after 30 minutes).

4) Flexural tests suggest that the compression yield strength exceeds the tensile yield strength.

5) Butt joint tensile strength exhibits a moderate bond thickness dependence. Joint strength decreases 20% as bond thickness increases from 0.025 to 0.100 inch.

6) The adhesive has a relatively high K_{IC} of about 2000 psi $in^{0.5}$.

7) ENF tests indicate that fatigue crack growth can occur at small fractions (<35%) of the Mode II energy release rate required to initiate cracking under monotonic loading.

REFERENCES

[1] Reedy, E. D., Jr. and Guess, T. R. "Tubular Lap Joints for Wind Turbine Applications: Test and Analysis," Proceedings 14th Annual Energy-Sources Technology Conference and Exhibition, Houston, TX, January 1991.

[2] Reedy, E. D., Jr. and Guess, T. R. "Composite-to-Metal Tubular Lap Joints: Strength and Fatigue Resistance," International Journal of Fracture, Vol. 63, 1993, pp. 351-367.

[3] Guess, T. R., Reedy, E. D., Jr., and Slavin, A. M., "Testing Composite-to-Metal Tubular Lap Joints," to be published in Journal of Composites Technology and Research.

[4] Reedy, E. D., Jr. and Guess, T. R. "Comparison of Butt Tensile Strength Data with Interface Corner Stress Intensity Factor Prediction," International Journal of Solids and Structures, Vol. 30, 1993, pp. 2929-2936.

[5] Reedy, E. D., Jr. and Guess, T. R. "Butt Tensile Joint Strength: Interface Corner Stress Intensity Factor Prediction," To appear in Journal of Adhesion Science and Technology, 1995.

[6] Carlsson L. A., and Pipes, R. B. Experimental Characterization of Advanced Composite Materials, Prentice-Hall, Inc., Englewood Cliffs, New Jersey, 1987, pp. 159-171.

Table 1. Hysol EA-9394 adhesive tensile moduli at a strain rate of 0.0003s^{-1}.

SPECIMEN ID	MODULUS (10^6 psi)
9394_T1	0.61
9394_T2	0.60
9394_T3	0.62
9394_T4	0.60
9394_T5	0.62
9394_T6	0.61
9394_T7	0.61
Average=	0.61
St dev=	0.01
cv (%)=	1.36

Table 2. Hysol EA-9394 adhesive compression static and stress relaxation results.

SPECIMEN ID	STRAIN RATE (1/s)	PEAK STRESS (psi)		INITIAL MODULUS (10^6 psi)	INITIAL POISSON'S RATIO
		INITIAL	2ND LOADING AFTER 30 MINUTE HOLD		
9394_2	.00300	11,400	12,400	0.54	0.40
9394_1	.00030	10,200	12,200	0.60	0.37
9394_3	.00003	9,250	12,000	0.62	0.37
RELAX1	.00030	—	—	0.54	—
RELAX2	.00030	—	—	0.64	—
RELAX3	.00030	—	—	0.63	—
			Average=	0.59	
			St dev=	0.04	
			cv (%)=	7.4	

Table 3. Hysol EA-9394 adhesive four-point flexural results.

SPECIMEN ID	INITIAL FLEX MODULUS (10^6 psi)		POISSON'S RATIO	
	COMPRESSION SIDE	TENSION SIDE	COMPRESSION SIDE	TENSION SIDE
9394_B1	0.68	0.65	0.37	0.34
9394_B2	0.71	0.68	----	----

Table 4. Hysol EA-9394 static and stress rupture butt tensile results.

STATIC FAILURE TESTS

Specimen Number	Bond Thickness (in)	Nominal Failure Stress (psi)
1	.025	6550
2	.024	7390
3	.022	7560
4	.024	7900
5	.023	6940
6	.024	7400
7	.024	5720
8	.023	5180
avg		6830
stdev		953
cv		14.0%
9	.048	5160
11	.049	6250
13	.051	6820
15	.049	6550
17	.048	5970
19	.048	5950
21	.049	5710
23	.050	5060
avg		5934
stdev		619
cv		10.4%
25	.102	5650
27	.113	5400
29	.101	4780
31	.100	5270
33	.100	5330
35	.099	5260
37	.099	6000
39	.098	5540
avg		5404
stdev		352
cv		6.5%

STRESS RUPTURE TESTS

Specimen Number	Bond Thickness (in)	Stress Level (psi)	Percent of Static Failure Load (%)	Time @ Break or Added load (hr)	Residual Strength (psi)
18	.045	4375	74	3.5*	6150
10	.049	4375	74	3.66*	6450
12	.049	4375	74	21.7*	7080
14	.048	4850	82	2.9	
16	.047	4850	82	6.8*	6700
20	.049	4850	82	2.1	
32	.098	4375	81	3.9*	5120
34	.098	4375	81	2.9	
38	.099	4375	81	0.24	
30	.099	4850	90	failed during loading	
36	.099	4850	90	0.92	
40	.096	4850	90	0.006	

* Specimen did not fail during stress rupture; residual strength measured at this time.

17

Table 5. Summary of ENF 3-point bend fracture toughness test results for Hysol EA-9394 adhesive.

Sample ID	Avg. Crack Length (in)	r=a/w	f (r)	Pmax (lb)	K_{Ic} (psi*in^{-5})
EA9394-1	0.102	0.204	1.188	68.0	1956
EA9394-2	0.081	0.163	1.057	74.3	1902
EA9394-3	0.074	0.148	1.011	76.5	1878
EA9394-4	0.114	0.229	1.268	62.0	1910
EA9394-5	0.062	0.125	0.936	78.5	1779
EA9394-6	0.129	0.258	1.368	59.8	1980
EA9394-7	0.074	0.148	1.010	98.8	2417
				Average	1975
				St dev	205
				cv (%)	10

Table 6. Summary of static ENF Mode II fracture toughness tests. (Critical Gc based on peak load).

GROUP	SPECIMEN ID	SPECIMEN ORIENTATION	CRACK INITIATION METHOD	Gc (J/m^2)	OBSERVED FAILURE
1	ENF-21	Composite side down	See Note 1	735	Cracking observed in both composite & along metal/adhesive interface. When pried open, specimen parted at metal/adhesive interface, but had crack in 1st ply of composite. Crack in only part way thru width of composite which still had integrity.
1	ENF-24	Composite side down	See Note 1	430	Precrack appeared to be in composite, but in test crack started at top of interface @ corner of notch. Metal/adhesive interface failure.
2	ENF-22	Composite side up	See Note 1	825	Precrack appeared to be in composite. Precrack widened but did not extend. Failure at metal/adhesive interface. Some compression failure under load ram.
3	ENF-23	Composite side down	See Note 2	1140	Precrack appeared to be in composite. Crack grew in composite. Composite failure.
4	ENF-25	Composite side up	See Note 2	1270	Precrack appeared to be in composite. Crack growth abrupt in composite. Composite failure.
5	ENF-33	Composite side up	See Note 3	655	Failed in composite (surface resin and small amount of fiber) took off top layer of ployester.
5	ENF-42	Composite side up	See Note 3	1100	Failed in composite (surface resin and small amount of fiber) took off top layer of ployester.
5	ENF-27	Composite side up	See Note 3	690	Failed in composite (surface resin and small amount of fiber) took off top layer of ployester.
6	ENF-31	Composite side down	See Note 3	600	Failed at EA-9394/aluminum interface: adhesive failure
6	ENF-38	Composite side down	See Note 3	655	Failed at EA-9394/aluminum interface: adhesive failure; small amount of failure in 1st layer composite on one side.
6	ENF-39	Composite side down	See Note 3	265	Failed at EA-9394/aluminum interface: adhesive failure

Note 1. Saw cut in bondline then wedged open to start initial natural crack.
Note 2. No saw cut; bondline wedged open to start initial natural crack.
Note 3. Saw cut in bondline then specimen fatigued in 3-point bend to grow initial natural crack.

19

Table 7. Summary of static and fatigue ENF results

SPECIMEN	TYPE TEST	G (J/m^2)	NUMBER OF CYCLES, N	COMMENT
ENF-33	STATIC	689	1	To failure on initial loading cycle
ENF-42	STATIC	1157	1	To failure on initial loading cycle
ENF-27	STATIC	726	1	To failure on initial loading cycle
ENF-32	FATIGUE	202	80,000	Runout (no crack extension)
ENF-32B	FATIGUE	247	36,000	Runout (no crack extension)
ENF-37	FATIGUE	247	60,000	Runout (no crack extension)
ENF-37B	FATIGUE	293	33,000	Runout (no crack extension)
ENF-30	FATIGUE	293	9,500	0.10 inch crack extension
ENF-32C	FATIGUE	293	63,000	0.10 inch crack extension
ENF-37C	FATIGUE	343	80,000	0.10 inch crack extension
ENF-37D	FATIGUE	459	50,000	0.10 inch crack extension

Note: 5 Hz cycle rate, composite side up and fatigue pre-crack.
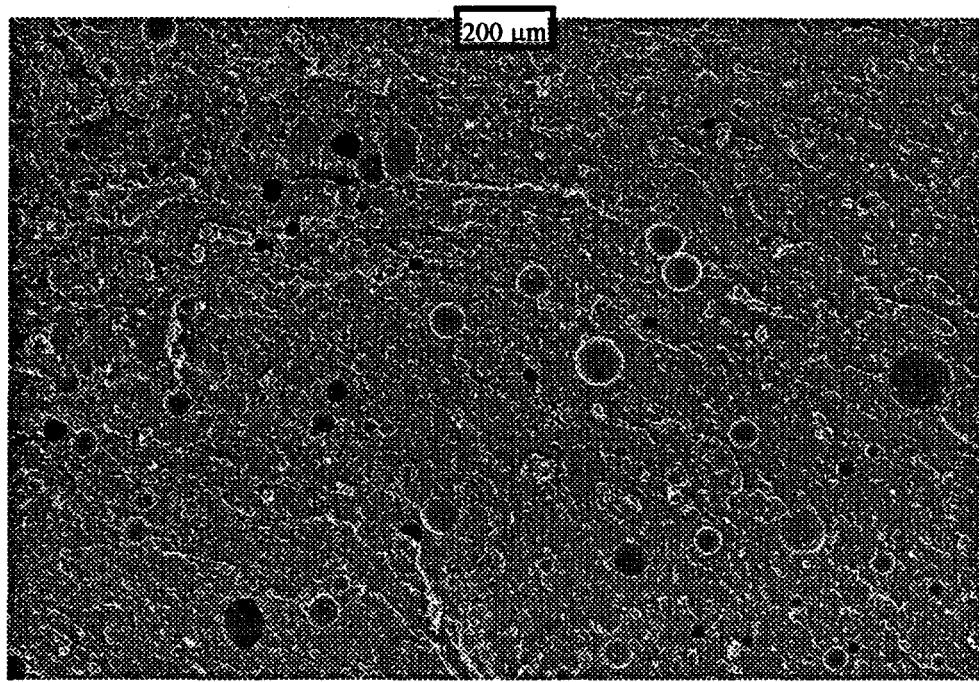
Figure 1. SEM of EA-9394 adhesive showing porosity distributed throughout the material.
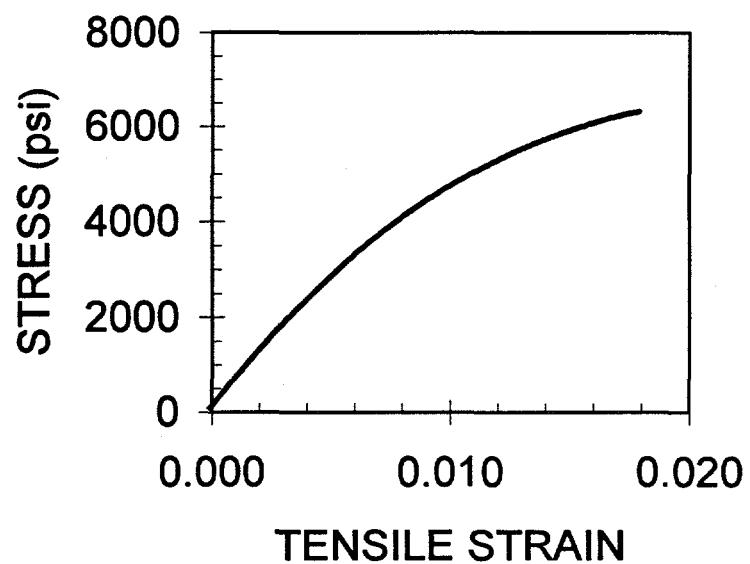
Figure 2. Typical tension stress-strain response of Hysol EA-9394 adhesive.
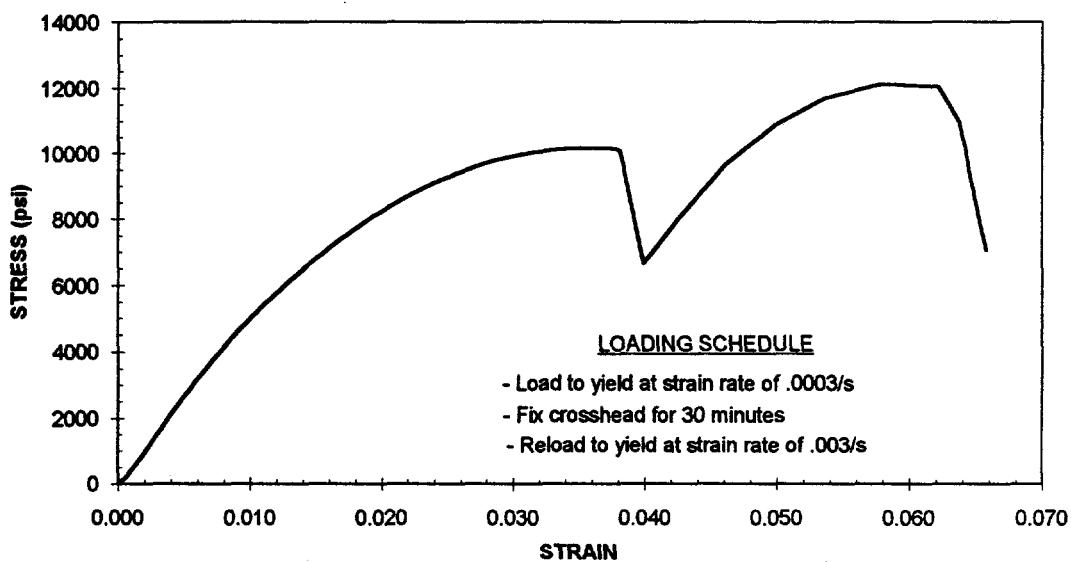
Figure 3. Compression stress relaxation stress-strain response of Hysol EA-9394 adhesive.
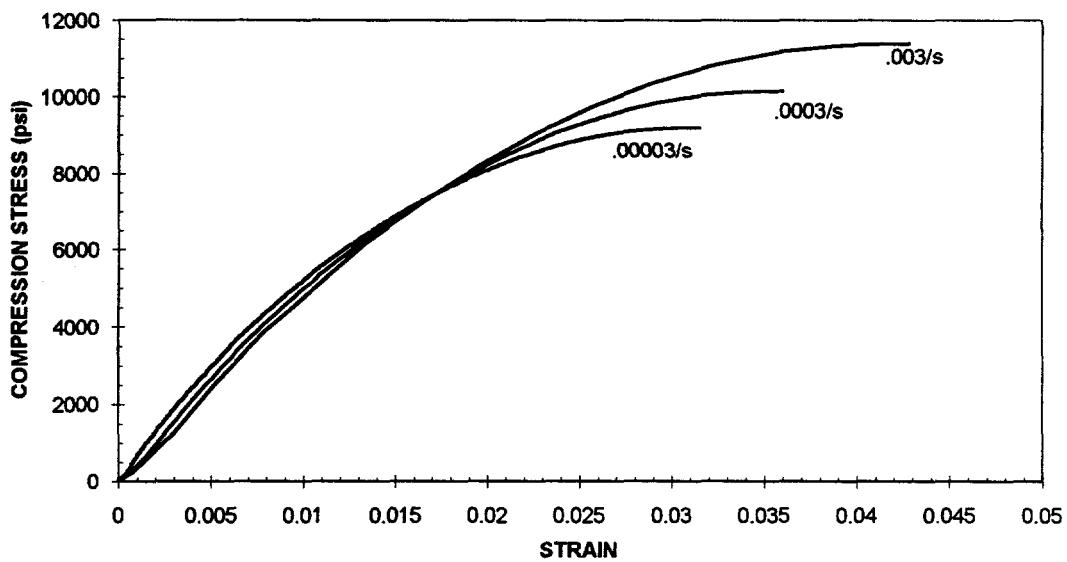

Figure 4. Compression stress-strain response of Hysol EA-9394 adhesive at three strain rates.
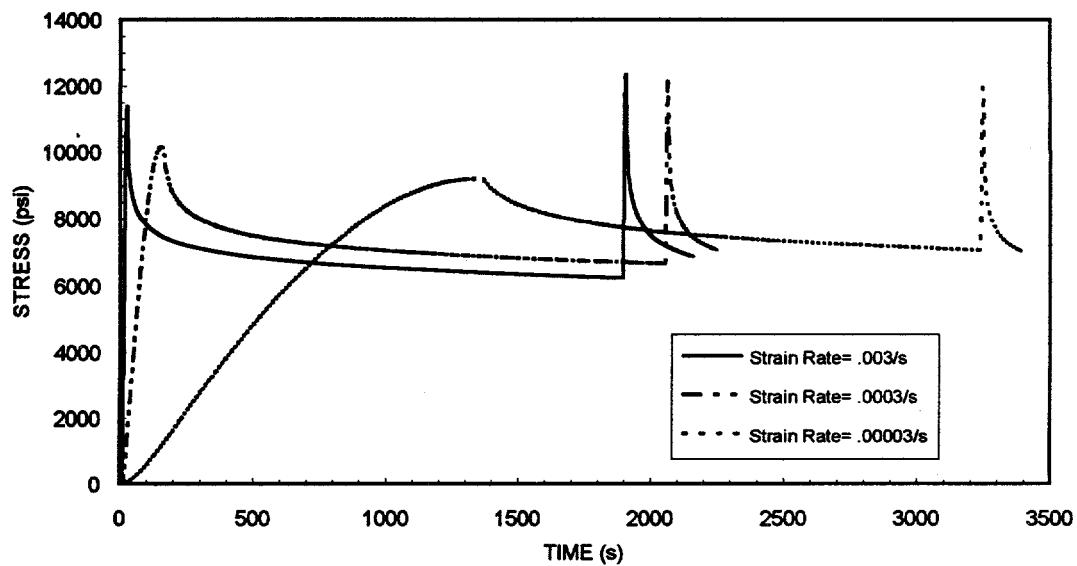
Figure 5. Compression stress relaxation responses of Hysol EA-9394 adhesive for three initial loading strain rates. Strain rate of 0.003 s^{-1} on second loading of each specimen.
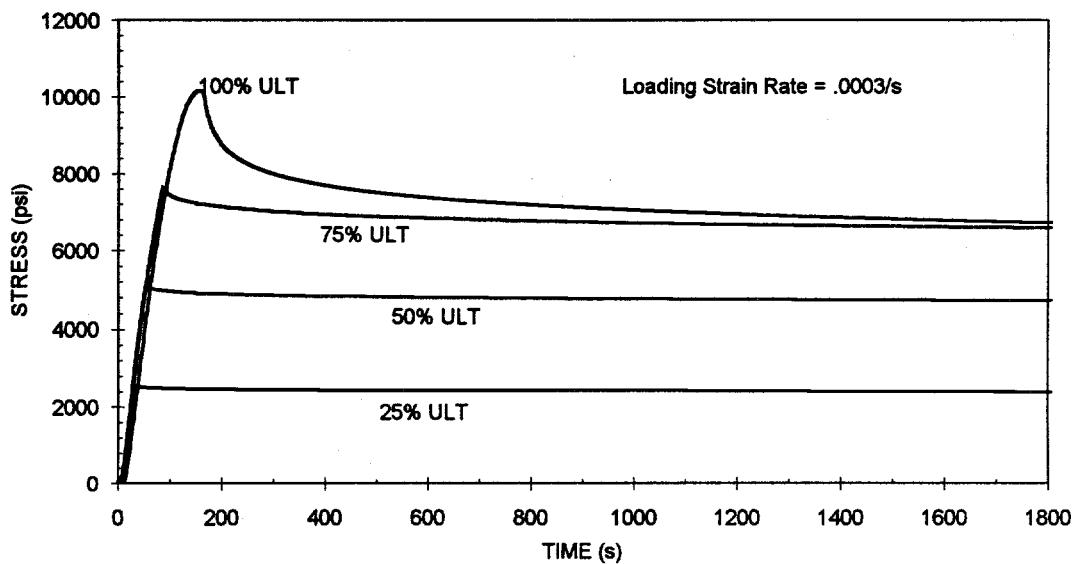
Figure 6. Compression stress relaxation responses of Hysol EA-9394 adhesive with initial loading to different levels of yield strength.
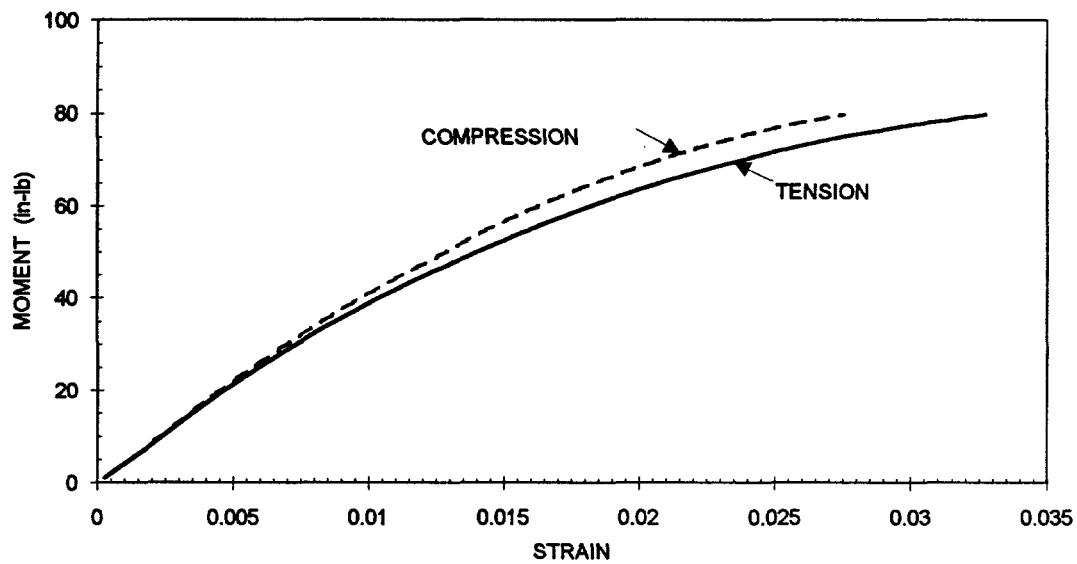
Figure 7. Typical flexural moment-strain response of of Hysol EA-9394 adhesive.
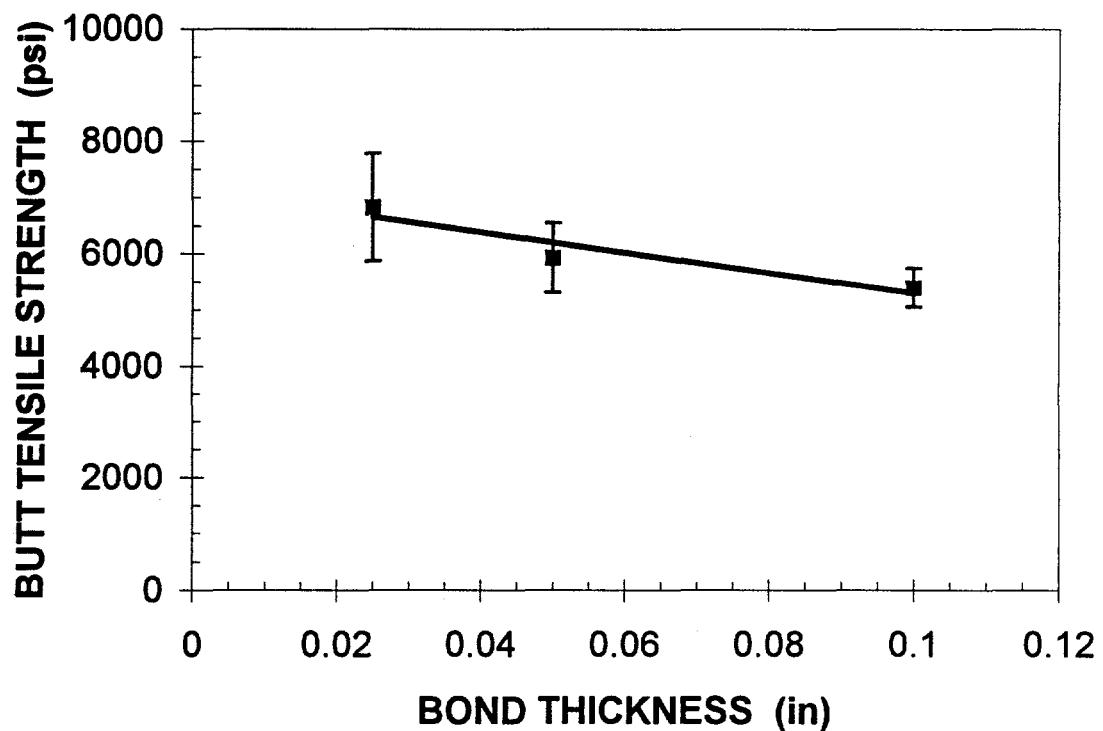
Figure 8. Butt joint tensile strength versus bond thickness for Hysol EA- 9394 adhesive cured and tested at room-temperature.
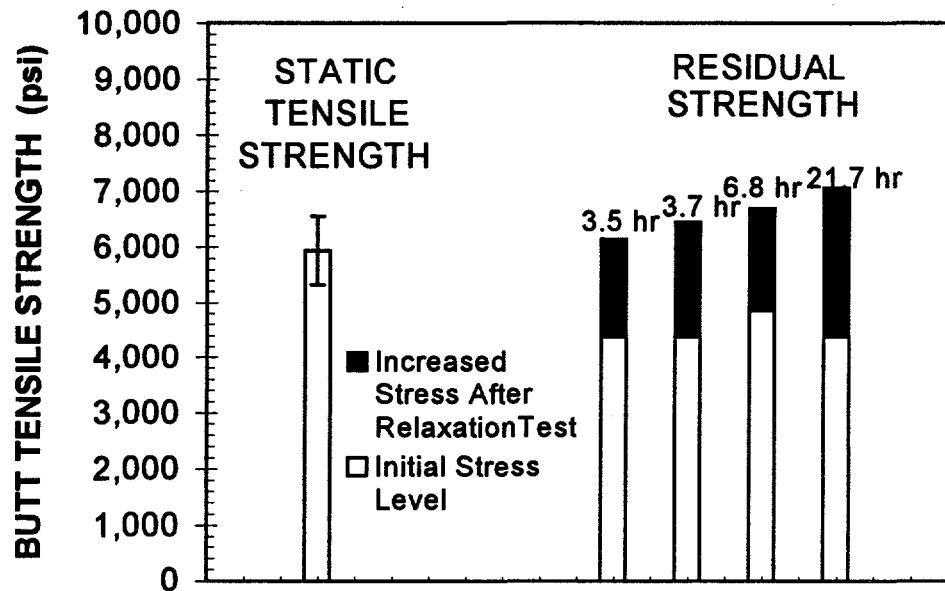
Figure 9. Butt tensile joints subjected to static tensile tests and stress rupture tests. The times refer to the time of sustained load prior to loading specimen to failure for residual strength. Nominal bondline thickness of 0.05 inch.
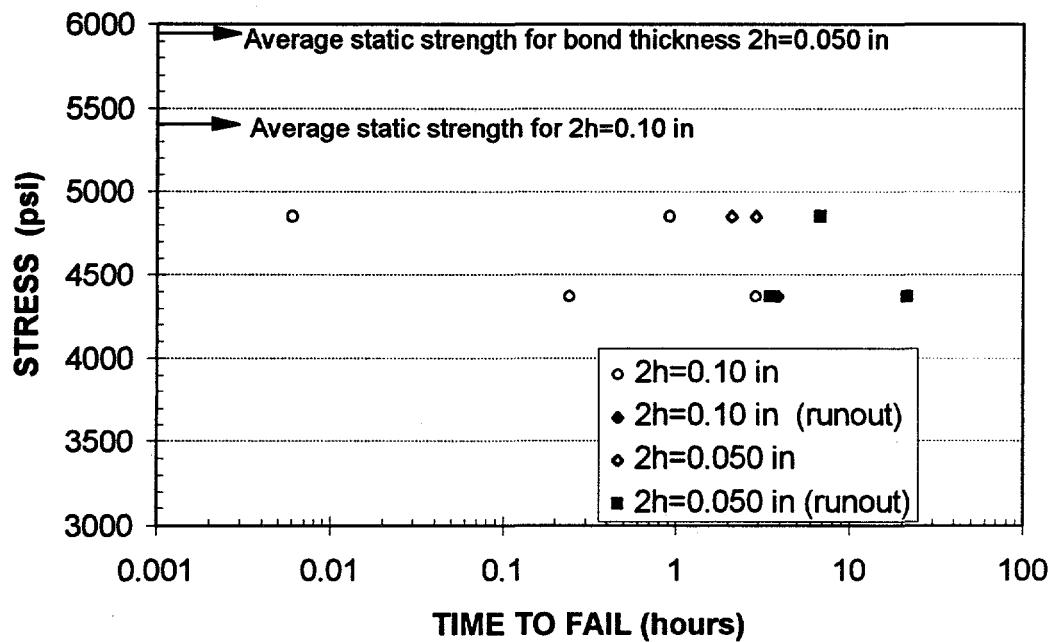

Figure 10. Time to fail (or runout) of butt tensile joints subjected to sustained loading at a stress below the static strength. Runout means specimen did not fail during the stress rupture test. Nominal bondline thicknesses of 2h =0.05 and 0.10 inch.
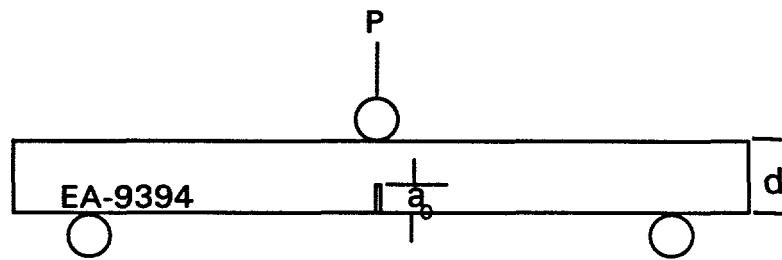
Figure 11. Three-point bend Single-Edge-Notch (SEN) fracture toughness specimen.
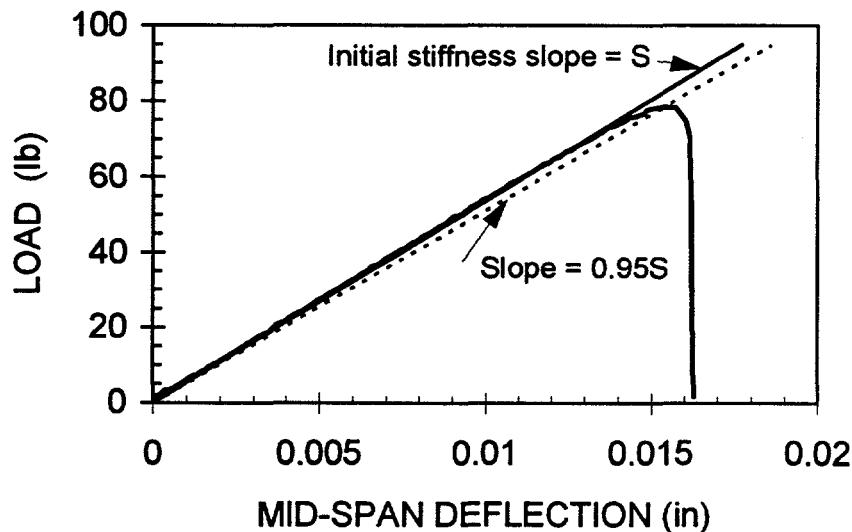
Figure 12. Load-deflection response of SEN three-point bend fracture toughness test on bulk Hysol EA-9394 adhesive.
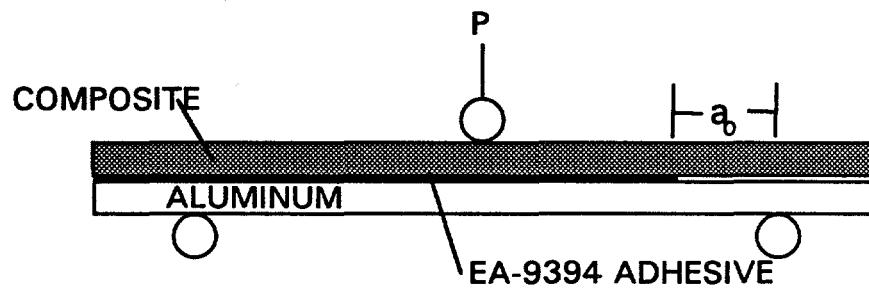
Figure 13. Three-point bend End-Notch Flexure (ENF) fracture toughness specimen.
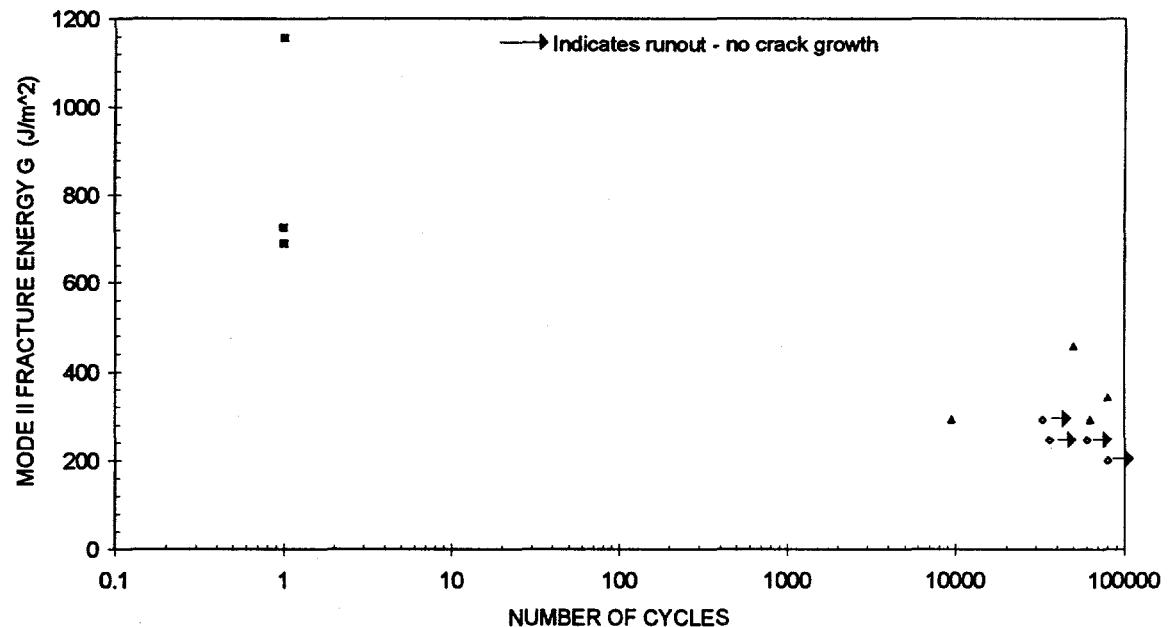
Figure 14. Mode II shear strain energy of bimaterial ENF specimens with Hysol EA-9394 adhesive bondline.

27

UNLIMITED RELEASE:

R. E. Akins
Washington & Lee University
P.O. Box 735
Lexington, VA 24450

H. Ashley
Dept. of Aeronautics and
  Astronautics Mechanical Engr.
Stanford University
Stanford, CA 94305

B. Bell
FloWind Corporation
990 A Street
Suite 300
San Rafael, CA 94901

C. P. Butterfield
NREL
1617 Cole Boulevard
Golden, CO 80401

G. Bywaters
New World Power Technology Center
Box 659
Moretown, VT 05660-0659

R. N. Clark
USDA
Agricultural Research Service
P.O. Drawer 10
Bushland, TX 79012

C. Coleman
Northern Power Systems
Box 659
Moretown, VT 05660

O. Dyes
Wind/Hydro/Ocean Div.
U.S. Department of Energy
1000 Independence Avenue, SW
Washington, DC 20585

D. M. Eggleston
DME Engineering
P.O. Box 5907
Midland, TX 79704-5907

P. R. Goldman
Wind/Hydro/Ocean Division
U.S. Department of Energy
1000 Independence Avenue
Washington, DC 20585

I. J. Graham
Dept. of Mechanical Engineering
Southern University
P.O. Box 9445
Baton Rouge, LA 70813-9445

C. Hansen
University of Utah
Department of Mechanical Engineering
Salt Lake City, UT 84112

L. Helling
Librarian
National Atomic Museum
Albuquerque, NM 87185

S. Hock
Wind Energy Program
NREL
1617 Cole Boulevard
Golden, CO 80401

W. E. Holley
Kenetech Windpower
6952 Preston Avenue
Livermore, CA 94550

B. J. Im
McGillim Research
4903 Wagonwheel Way
El Sobrante, CA 94803

K. Jackson
Dynamic Design
123 C Street
Davis, CA 95616

C. Lange
Civil Engineering Dept.
Stanford University
Stanford, CA 94305

R. R. Loose, Director
Wind/Hydro/Ocean Division
U.S. Department of Energy
1000 Independence Ave., SW
Washington, DC 20585

R. Lynette
AWT/RLA
425 Pontius Avenue North
Suite 150

MS 9018   Central Technical Files, 8523-2
MS 0899   Technical Library, 13414 (5)
MS 0619   Print Media, 12615
MS 0100   Document Processing, 7613-2
For DOE/OSTI (2)

MS-0439   D. J. Segalman, 1434
MS 0827   P. J. Hommert, 1502
MS 0443   S. N. Burchett, 1517
MS 0443   R. S. Chambers, 1517
MS 0443   M. K. Neilsen, 1517
MS 0437   E. D. Reedy, 1518 (10)
MS 0437   R. K. Thomas, 1518
MS 0367   A. B. Adolf, 1812
MS 0960   J. Q. Searcy, 2400
MS 0961   J. A. Sayre, 2403
MS 0958   J. L. Ledman, 2472
MS 0958   J. A Emerson, 2472
MS 0958   D. L. Zamora, 2472
MS 0958   A. S. Baca, 2472
MS 0958   T. R. Guess, 2472 (10)
MS 0958   M. E. Stavig, 2472
MS 0958   H. W. Arris, 2472
MS 0958   M. W. Donnelly, 2472
MS 0958   J. A. Brammer, 2472
MS 0708   H. M. Dodd, 6214
MS 0708   H. J. Sutherland, 6214 (20)
MS 9403   J. Costa, 8711
MS 9404   L. Domeier, 8713